

Numerical Modeling Methodology for Strength Evaluation of Deep Bridge Bent Caps

Anish Sharma and Serhan Guner

Synopsis: Due to the increase in traffic and transported freight in the past decades, a significant number of in-service bridges have been subjected to loads above their original design capacities. Bridge structures typically incorporate deep concrete elements, such as cap beams or bent caps, with higher shear strengths than slender elements. However, many in-service bridges did not account for the deep beam effects in their original design due to the lack of suitable analysis methods at that time. Nonlinear finite element analysis (NLFEA) can provide a better assessment of the load capacity of deep bridge bent beams while accounting for the deep beam action. However, there is little guidance on how to conduct a numerical strength evaluation using the NLFEA. This study presents a nonlinear modeling methodology for the strength evaluation of deep bridge bents while considering advanced concrete behavior such as tension stiffening, compression softening, and dowel action. Five existing bridge bent beams are examined using the proposed methodology. The effectiveness and advantages of the proposed methodology are discussed by comparing the numerical results, including the load-displacement responses, load capacities, cracking patterns and failure modes, with the strut-and-tie and sectional analysis methods. Important modeling considerations are also discussed to assist practitioners in accurately evaluating deep bridge bents.

Keywords: bridge bent beams, deep beams, NLFEA, strength evaluation, safety assessment, failure, sectional method, strut-and-tie method, rehabilitation

INTRODUCTION

Bridge structures typically incorporate deep reinforced concrete elements, such as bents or cap beams. Increases in traffic and transported freight over the past decade have increased the loading on the existing bridge bents, which requires accurate strength evaluation methods for making repair and strengthening decisions. Reinforced beams are typically subjected to a combination of axial, flexural and shear stresses. The commonly used bending theory (i.e., the sectional method) is based on the Bernoulli hypothesis, which assumes a linear distribution of strains through the section depth. However, bridge bent beams often have their shear span-to-depth ratios (a/d) less than 2.5, which qualifies them as deep beams. The behavior of deep beams must be treated separately because they do not exclusively exhibit a linear strain distribution (Collins and Mitchell 1991; Schlaich and Shafer 1991; Schlaich et al. 1987; Rogowsky and MacGregor 1986). Experimental work conducted on deep beams demonstrated that diagonal shear cracking is their main governing behavior (Scott et al. 2012; Kim et al. 2011; Oh and Shin 2001; Tan et al. 1997; Kani 1967; Clark 1951). The strut-and-tie-method (STM) is shown to represent the behavior of deep beams better than the sectional method (Baniya and Guner 2019; Kim et al. 2011; Oh and Shin 2001; Kani 1967). Various empirical formulations and analytical methods were proposed for evaluating the shear strength of deep beams based on the strut-and-tie approach (Gandomi et al. 2013; Scott et al. 2012; Guner and Vecchio 2010; Quintero-Febres et al. 2006; Hwang and Lee 2002; Oh and Shin 2001). However, these methods do not take into account the nonlinear material behavior and have limitations in predicting the post-peak softening behavior of deep beams, which is required for the prediction of displacement ductility. The complexity and uniqueness of bridge bents require a more advanced analysis approach such as nonlinear finite element analysis (NLFEA).

Current advances in computational capabilities of finite element modeling have been proven a versatile tool for studying the nonlinear pre- and post-peak behavior of structural members (Alsaeq 2013; Özcan et al. 2009). NLFEA by its nature is a global type of assessment, in which all structural parts interact. It has been shown to accurately model the nonlinear strain distributions and the effects of shear cracking on the stress and strain fields (Pan et al. 2017; Demir et al. 2016; Barbachyn et al. 2012). Recent researchers have demonstrated the possibilities and advantages of NLFEA for accurately simulating the nonlinear behavior of deep beams, including the effects of shear cracking and the nonlinearity of the strain distribution (Salgado and Guner 2018a, 2018b; Pan et al. 2017; Demir et al. 2016; Barbachyn et al. 2012; Niranjana and Patil 2012). However, there is little guidance on how to use the results from NLFEA for determining the strength and safety of existing bridge bents.

This study proposes a strength assessment methodology for bridge bent beams based on a pushover analysis performed using NLFEA. To achieve an accurate strength evaluation, NLFEA modeling of the deep bridge bents accounts for a number of advanced material behaviors including concrete confinement, compression softening, tension stiffening and softening, and reinforcement dowel action and buckling. The methodology uses a pushover analysis and a two-stage safety assessment procedure to determine a reserve or overload percentage for each bridge bent. The overall modeling process is presented through a case study, involving five existing bridge bents, to assist practitioners in accurately evaluating the strength of bridge bents. The effectiveness of the proposed methodology, as compared to the sectional and strut-and-tie methods, is also discussed.

RESEARCH SIGNIFICANCE

Many in-service bridge bents did not account for deep beam effects in their original design. When analyzed using sectional methods, they are often found overloaded. NLFEA has the capabilities to capture the deep beam characteristics to more accurately predict the strength and ductility of deep bridge bents. However, there is a lack of methodologies on how to use the NLFEA, including the model development and the use of analysis results for the strength assessment of deep bridge bents. This study proposes a methodology using NLFEA and a two-stage safety assessment procedure to better interpret the holistic behavior and evaluate the strength of deep bridge bents.

NUMERICAL MODELING AND SAFETY ASSESSMENT METHODOLOGY

Finite element modeling

The proposed methodology uses a two-dimensional continuum-type finite element (FE) modeling approach. It can be applied using any FE modeling software on the condition that it is capable of simulating significant material behaviors including concrete confinement, compression softening, tension stiffening and softening, and reinforcement dowel action. The program VecTor2 (Wong et al. 2013) is used in this study, which employs a smeared, rotating crack model

based on the Modified Compression Field Theory (MCFT) (Vecchio and Collins 1986) and the Distributed Stress Field Model (DSFM) (Vecchio 2000). The MCFT has been adopted by the AASHTO (2017) and CSA A23.3 (2014) codes. VecTor2 has been shown to provide an accurate simulation of the experimental behaviors in terms of strength, crack patterns, and the flow of principal stresses (Baniya et al. 2018; Senturk and Higgins 2010a). The graphical pre-processor, Formworks Plus (Wong et al. 2013), is used to create numerical models while the post-processor Augustus is used to visually examine the analysis results.

The concrete is modeled using 8-degree-of-freedom quadrilateral elements in geometrically uniform regions or 6-degree-of-freedom triangular elements in geometrically non-uniform regions as shown in Figures 1(a) and 1(b). The shear reinforcement is smeared into the concrete regions and the longitudinal reinforcement is discretely modeled as trusses through two-node elements with 2-degrees-of-freedom per node as shown in Figure 1(c).

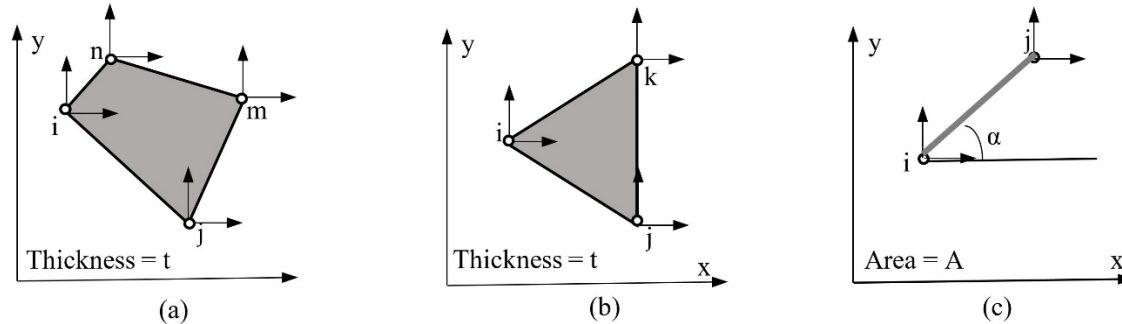


Fig. 1—(a) Quadrilateral element for concrete, (b) triangular element for concrete, and (c) truss bar element for rebar

The NLFEA incorporates several advanced material behaviors specific to cracked reinforced concrete, as listed in Table 1. For deep bridge bents, four of these behaviors were found to be significant: concrete compression and tension softening, dowel action, and tension stiffening (Figure 2). Concrete compression softening is the reduction in the uniaxial compressive strength and stiffness due to transverse tensile cracking. The concrete tension softening, on the other hand, reduces the effectiveness of the concrete struts due to significant shear cracking that occurs when low amounts of stirrup reinforcement are present, which has been noticed in many bent beams. In addition, these low amounts of stirrups reduce the shear capacity such that the additional shear resistance due to dowel action becomes important. Finally, due to a lack of well-distributed layers of reinforcement in many older bent beams, they may exhibit flexural cracking, requiring the modeling of concrete tension stiffening effects.

Table 1—Material models included in VecTor2

| Material behavior | Model |
|-----------------------|--------------------------|
| Compression softening | Vecchio 1992-A |
| Tension stiffening | Modified Bentz 2003 |
| Tension softening | Linear |
| Rebar dowel action | Tassios (Crack slip) |
| Rebar buckling | Refined Dhakal-Maekawa |
| Crack width check | Max crack width of Agg/5 |
| Confinement strength | Kupfer/Richart |

Popovics (1973) and Modified Park-Kent (Bunni et al. 1982) models are employed for the pre- and post-peak response of the concrete, respectively. Even though the proposed methodology includes a static pushover analysis, the concrete model includes nonlinear hysteresis as shown in Figure 2(a) because some parts of the bridge bents will unload and reload, which is when the cracking of concrete and the yielding of reinforcement occurs. The stress between the concrete and reinforcement is transferred through the perfect bond. The steel reinforcement stress-strain response is composed of linear-elastic response, a yield plateau, and rupture in tension as shown in Figure 2(b). Buckling of steel reinforcing is also taken into account (Akkaya et al. 2019).

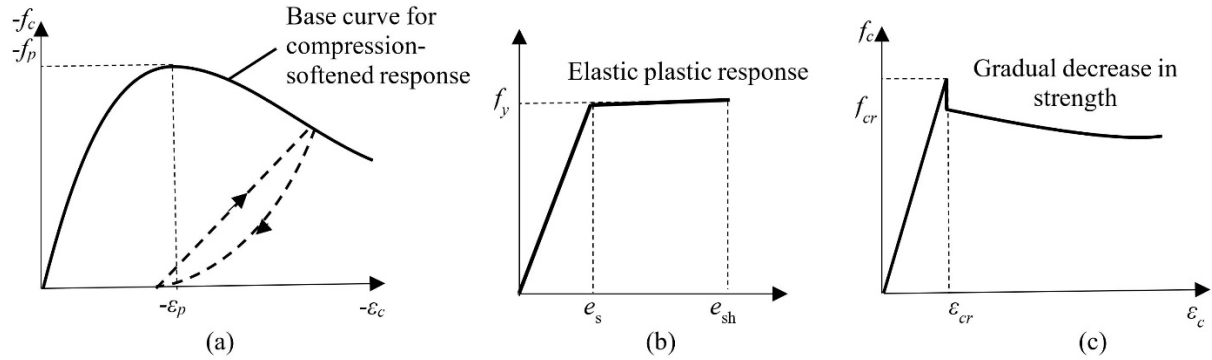


Fig. 2—(a) Concrete and (b) reinforcing steel material constitutive models, (c) tension stiffening response

Multiple concrete regions are created to represent different smeared reinforcement conditions; Figure 3 shows an example. The reinforcement ratio (ρ_t) for each concrete region having a cross-sectional area of out-of-plane reinforcement (A_b), number of stirrups leg (n), spacing (S_t), and width of the cross-section (W_c), is calculated using Eqn. 1. The symmetry of the pier cap allows for modeling one-half of the beam, which reduces the analysis time. Rollers are defined at the axis of symmetry and pin supports are defined at the lowest ends of the pier (not shown in Figure 3). Since no lateral load is considered, no significant stresses are developed in the column region and its effect can be neglected. Hence, the beam-column is considered monolithically jointed.

$$\rho_t = \frac{nA_b}{S_t W_c} \quad (1)$$

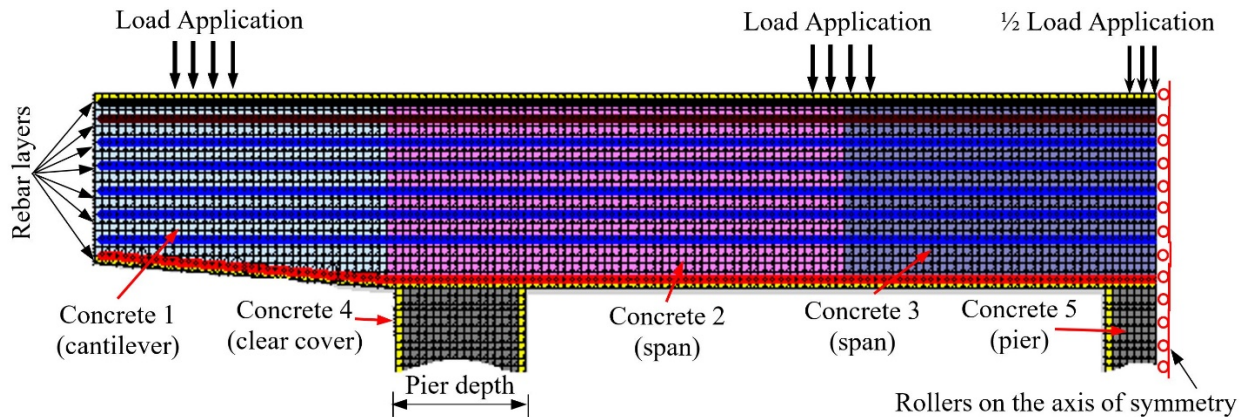


Fig. 3—FE model developed for NLFEA

For the load application, the dead load is applied fully and then the live load is applied uniformly up to the failure of the beam. Maximum displacement is recorded. For bridge bent beams with a cantilever span, maximum displacement usually occurs at the tip of the cantilever span, whereas for bridge bent beams with no cantilever span, it occurs at the inner mid-span. A load-displacement curve can be generated so the load causing the failure of the bent beam can be determined.

Experimental verification of modeling approach

The accuracy of the proposed material modeling approach was verified with the results from experiments conducted on six full-scale in-service bridge bents by Senturk and Higgins at Oregon State University (Senturk and Higgins 2010b; Senturk 2008). These bridge bents resemble conventionally reinforced concrete deck girder (RCDG) bridges built in the 1950s. Five specimens had an overall height of 72 in. (1829 mm) and one specimen had an overall height of 48 in. (1219 mm). The width of the bent caps is 16 in. (406 mm). The support reaction and the location of the applied loads were the same for all specimens. The experimental results from two bridge bents were used to verify the cracking patterns and load-displacement responses determined from the proposed modeling approach. The details of the experimental setup and material properties were discussed by Senturk (2008). In short, the first specimen

(originally referred to as D6.A2.G40#4.S) had a height of 72 in. (1829 mm), concrete strength of 3.52 ksi (24.4 MPa), reinforcing steel of yield strength 68.3 ksi (470 MPa), ultimate strength of 112.9 ksi (778 MPa), and #4 (13 mm) stirrups. For the second specimen (originally referred to as D4.A2.G40#4.S), the height of the beam was 48 in. (1219 mm) while the material properties were the same as for the first specimen.

The FE models of both specimens are shown in Figure 4. One-half of the beam was modeled and rollers were provided on the axis of symmetry. Top and bottom reinforcement were modeled as truss elements and the shear reinforcement was smeared in the concrete. Material models listed in Table 1 were used. Figure 4 shows the cracking conditions experimentally obtained (Senturk and Higgins 2010b; Senturk 2008) and numerically generated by the FE model. The shear cracking spanned from the support to the load application point, which indicated typical deep beam strut action. The FE model successfully captured the experimentally observed shear compression failure response as well as the strut action for both cases as shown in Figure 4.

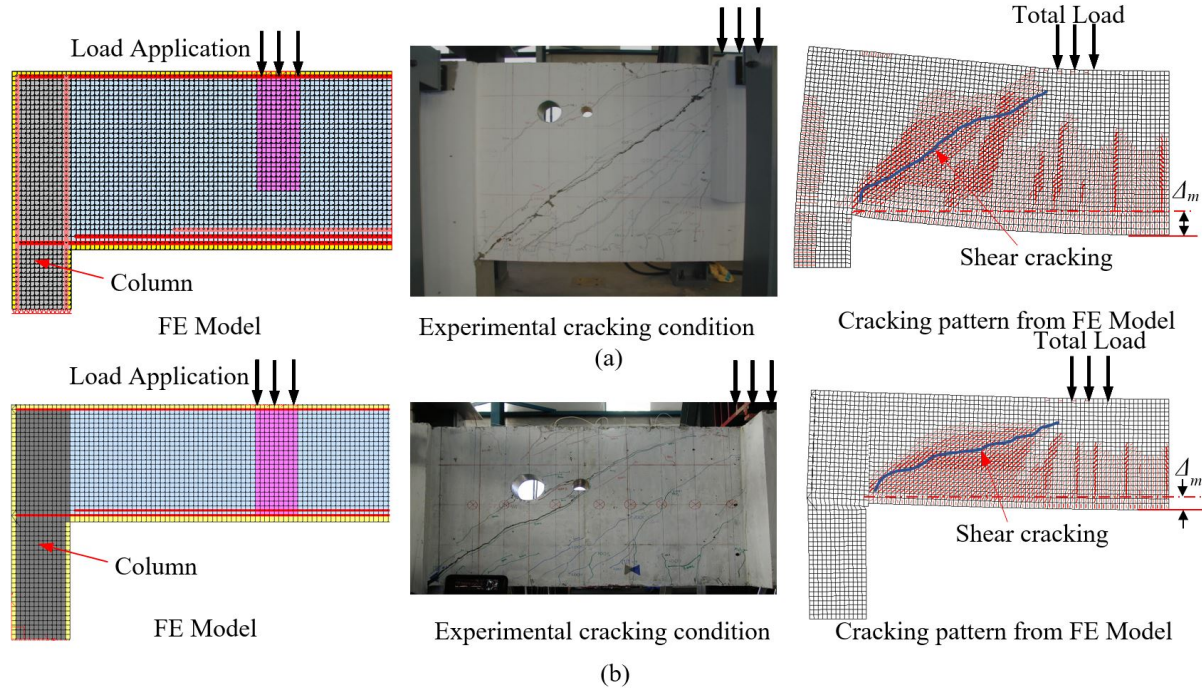


Fig. 4—FE model and cracking conditions for (a) D6.A2.G40#4.S and (b) D4.A2.G40#4.S

Figure 5 shows the total load and mid-span displacement (Δ_m) response experimentally obtained (Senturk and Higgins 2010b; Senturk 2008) and numerically calculated by the FE model. The peak load, peak displacement and overall stiffness response of both beams were well captured by the FE model. The FE analysis to experimental ratios of the peak load capacity were 10% on average for the specimens.

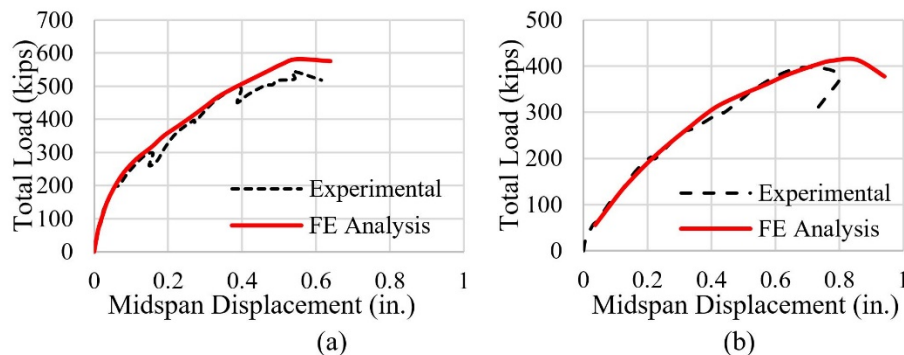


Fig. 5—Load-displacement response for (a) D6.A2.G40#4.S and (b) D4.A2.G40#4.S; 1 in. = 25.4 mm and 1 kip = 4.45 kN

Two-stage safety assessment

The safety requirements for structural design require that the resistance of the structure exceed the demand of the total applied loads. The performance of a bridge depends on the uncertainties in loads and material resistances. NLFEA simulates a global response of the bridge bent beams. Thus, the NLFEA results require a safety assessment to be determined for the strength evaluation of bent beams. Many design codes, such as AASHTO (2017), consider the uncertainties in loads and material resistance by load and resistance factors. These safety factors are intended for the linear-elastic sectional analysis. If used in nonlinear analysis, they may change the stress distribution, failure mode, and overall response. Hence, a new two-stage safety assessment procedure is proposed in this study for nonlinear analysis as outlined in Figure 6.

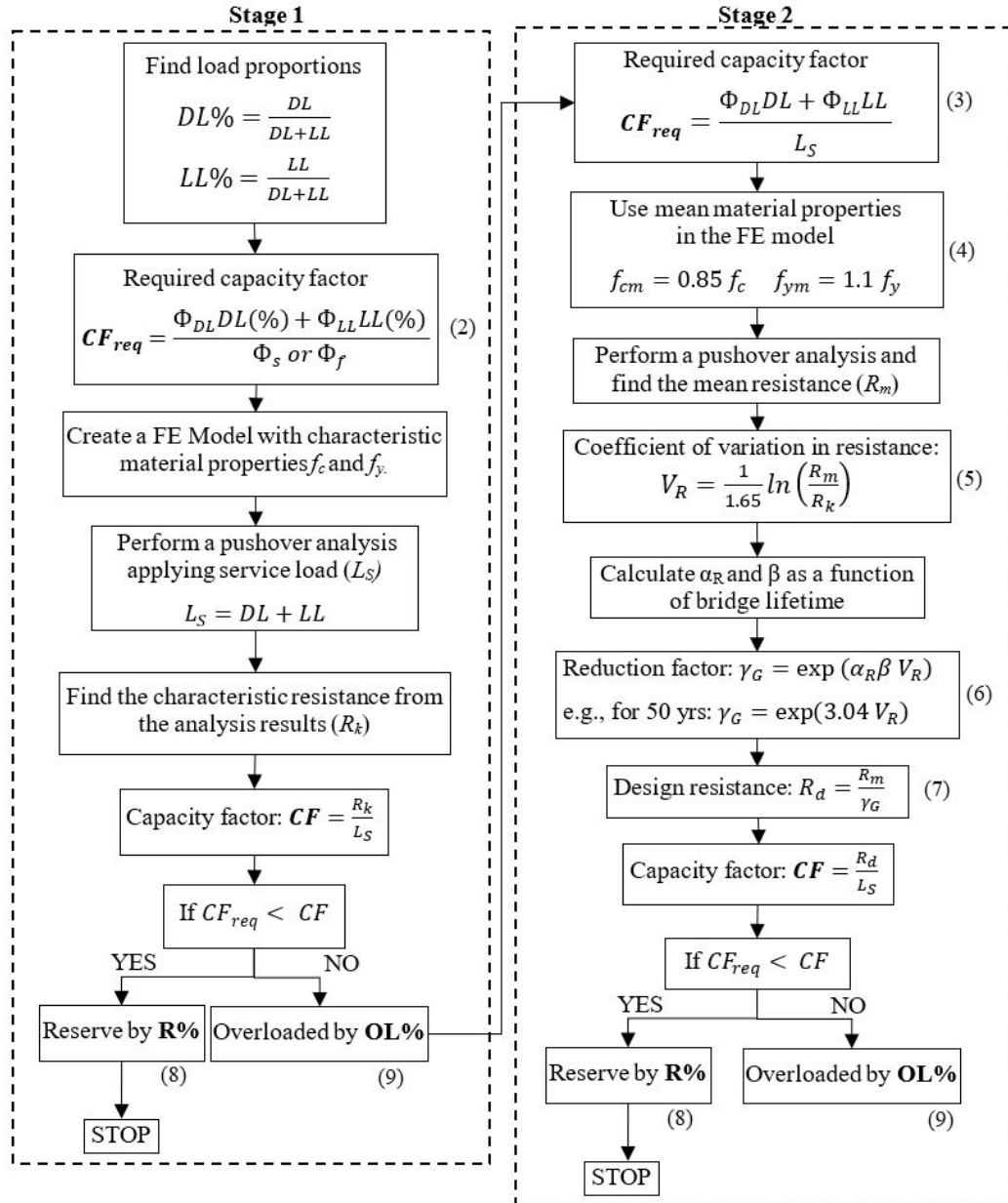


Fig. 6—Proposed methodology for the two-stage safety assessment of bridge bents using NLFEA

As summarized in Figure 6, the goal of the two-stage safety assessment is to find the required and actual capacity factors of the bridge beam. Stage 1 considers both the load and material resistance factors in the determination of the required capacity factor. This stage is simple to perform, requiring a single pushover analysis with characteristic (i.e.,

nominal) material properties. Stage 2 does not consider the material resistance factors when determining the required capacity factor; these factors are taken into consideration more precisely and probabilistically in the FE model. Compared to Stage 1, Stage 2 is more involved and requires two pushover analyses: one with the characteristic material properties and another with the mean material properties. Stage 2 assessment is only required if the bridge is found overloaded in Stage 1.

In Stage 1, the proportion of the dead load (DL) and live load (LL) with respect to the total load is determined first. Then, the load combination from the AASHTO (2017) specifications is followed to determine the factored load proportions to be used in Eqn. 2 (shown in Figure 6). Any other code specifications may be used depending on the location of the structure. The factored load is divided by the shear reduction factor (Φ_s) or flexural reduction factor (Φ_f) to determine the required capacity factor (CF_{req}) for the bridge bent beam as defined in Eqn. 2. The choice of material reduction factor depends on the mode of failure of the structure (ACI 318-19). The bridge bent beam is modeled in an FE software with characteristic material properties. The pushover analysis is then performed applying the service load (L_s), where total DL is applied initially and LL is applied uniformly until failure of the beam. The resistance (R_k in Figure 6) is determined from the load-displacement (i.e., pushover) curve. The actual capacity factor (CF), is determined as the ratio between R_k and the service load (L_s). If it is higher than the required capacity factor, the bridge bent is classified as safe. Otherwise, it is overloaded and a Stage 2 assessment should be made.

In Stage 2, the required capacity factor is determined as the ratio between the factored loads and L_s as defined in Eqn. 3 (shown in Figure 6). A comparison of Eqns. 2 and 3 shows that the material resistance factors are not used while determining the required capacity factor in Stage 2. This stage requires another NLFEA using mean material properties. For this, the mean yield strength of steel (f_{ym}) and the mean compression strength of concrete (f_{cm}) are estimated from the characteristic concrete compressive strength (f_c) and steel yield strength (f_y) as defined in Eqn. 4 (shown in Figure 6) (Cervenka 2008). A second pushover analysis is then performed to find the mean resistance (R_m) of the beam. The coefficient of variation of the resistance (V_R) is then calculated using Eqn. 5, where R_k and R_m are the resistances of the element using its characteristic and mean properties of materials, respectively. A reduction factor (γ_G) is probabilistically obtained using Eqn. 6, which is based on the sensitivity factor for the resistance reliability (α_R) and the reliability index (β), factors that depend on the service life of the bridge as shown in Figure 7(a). For a service life of 50 years, recommended values for the ultimate limit states are 0.8 and 3.8, respectively (Cervenka 2008). For a service life of 75 years, α_R and β are 0.8 and 3.2, respectively. Similarly, AASHTO (2017) recommends β of 3.5 for bridges. The sensitivity of γ_G with respect to service life is shown in Figure 7(b), which indicates differences below 5% for 50 or 75 years of structural service life. In this study, the reduction factor was calculated considering a service life of 50 years. The design resistance (R_d) is then obtained using the mean resistance (R_m) and γ_G as defined in Eqn. 7. The CF is determined as the ratio between R_d and L_s . If CF is more than CF_{req} , the bridge bent beam is considered safe; otherwise, it is considered overloaded.

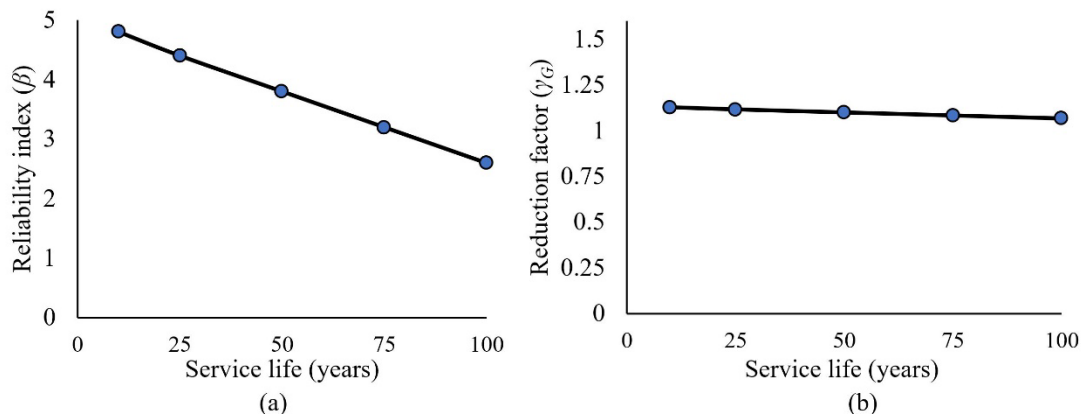


Fig. 7—(a) Reliability index versus service life and (b) reduction factor versus service life

The reserve capacity ($R\%$) and the overload capacity ($OL\%$) of the bridge bent beams can be determined at any stage using Eqns. 8 and 9, respectively.

$$R\% = \left(\frac{CF}{CF_{req}} - 1 \right) \times 100 \quad (8)$$

$$OL\% = \left(1 - \frac{CF}{CF_{req}} \right) \times 100 \quad (9)$$

APPLICATION OF THE PROPOSED METHODOLOGY

To demonstrate the application of the proposed methodology, five bent beams (four with and one without cantilever spans) of existing bridges were modeled with details listed in Table 2. The concrete characteristic compressive strengths for these beams ranged from 4 to 4.5 ksi (27.6 to 31 MPa); the number of piers ranged from three to seven; beam depths (d) ranged from 36 to 48 inches (915 to 1220 mm); and the shear span-to-depth ratios (a/d) ranged from 0.10 to 3.03; hence, most spans qualified as deep beams. The steel reinforcement characteristic yield stress was 55 ksi (378 MPa). As an example, the configuration and NLFEA model of Bridge 1 is shown in Figures 8 and 9, respectively.

Table 2—Bridge bent details; 1 ft = 304.8 mm and 1 in.² = 645.2 mm²

| Bridge | w (ft) | d (ft) | t (ft) | a/d | | A_y (bottom) (in. ²) | A_y (top) (in. ²) |
|----------|----------|----------|----------|-------|------|--|---------------------------------------|
| | | | | Min | Max | | |
| Bridge 1 | 44 | 4 | 3 | 1.40 | 1.89 | 7.00 | 13.95 |
| Bridge 2 | 51.17 | 3.5 | 3.5 | 0.10 | 1.91 | 8.00 | 9.46 |
| Bridge 3 | 64.67 | 3.5 | 3 | 0.19 | 2.80 | 8.00 | 8.00 |
| Bridge 4 | 53.33 | 4 | 3 | 0.50 | 1.51 | 9.00 | 8.00 |
| Bridge 5 | 87 | 3 | 3 | 0.14 | 3.03 | 7.90 | 7.90 |

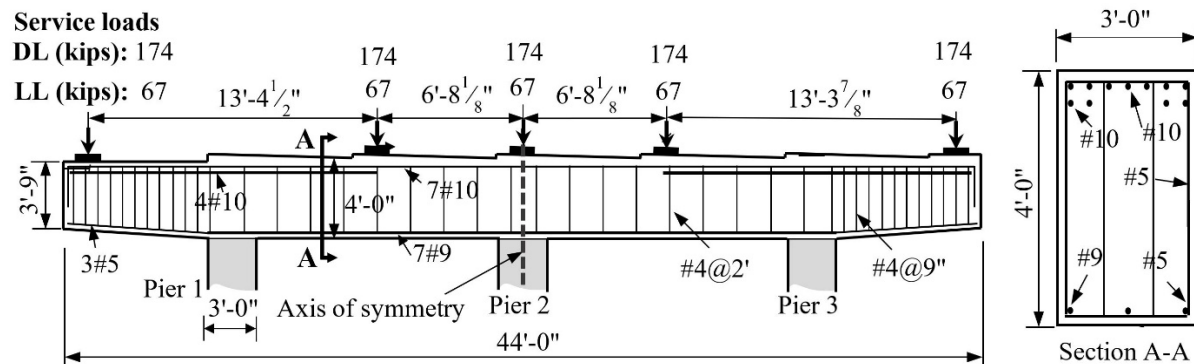


Fig. 8—Bridge 1 bent elevation and cross-section; 1 in. = 25.4 mm and 1 kip = 4.45 kN

The symmetry of the beams allowed for a one-half model, which significantly reduced the modeling effort and computation time. The lowermost ends of the columns were pinned while rollers were used on the axis of symmetry. Regions with different shear reinforcement are represented by different colors in Figure 9. The shear reinforcement in each region was calculated using Eqn. 1. A convergence test was performed for mesh size ranging from 20 to 100 mm. An FE mesh size of 50 x 50 mm satisfactorily balanced accuracy and computing time and hence, was used in modeling. Pushover analyses were performed with the total dead load applied initially; the live load was then increased in fixed increments of 10% until failure. The load-displacement responses were generated, and the strength evaluation was performed based on the proposed two-stage safety assessment procedure.

The sample beam shown in Figures 8 and 9 was originally designed using the Strength I ultimate load combination of $1.25DL + 1.75LL$ and the shear reduction factor (Φ_s) of 0.75 (ACI 318-19). Based on the load and material resistance factors, CF_{req} was determined to be 1.90 from Stage 1 assessment. An FE model was created with the characteristic material properties. The factored dead load of 217.5 kips was fully applied and then the live load was gradually applied until failure of the beam. From a single pushover analysis performed with characteristic material properties, R_k was determined to be 1456 kips (6480 kN). The CF of the bridge bent was determined to be 2.41, following the methodology discussed above [i.e., $1456 / [(174+67) \times 2.5]$]. The capacity factor was found to be higher than the

required, and the reserve capacity was calculated using Eqn. 8 to be 27% as shown in Figure 10(a). Since the bridge was found to be safe, there was no need to perform Stage 2 assessment. However, for demonstrative purposes, Stage 2 assessment was undertaken as follows.

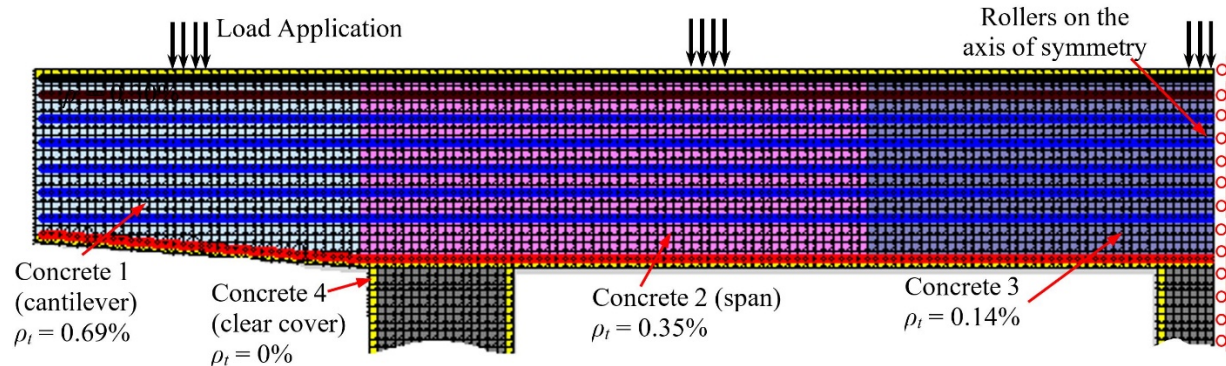


Fig. 9—FE model developed for Bridge 1

The required capacity factor in Stage 2 is determined as the ratio of the factored load to the service load, which was found to be 1.42 for the analyzed beam. The required capacity factor only considers uncertainties in load (i.e., load factors), while the FE model captures the material uncertainties. An additional pushover analysis was performed with the mean material properties as shown in Figure 10(b). The mean resistance was determined to be 1554 kips (6915 kN). As discussed above, the coefficient of variation and reduction factors were determined for 50 years of service life. The design resistance of the cap beam was then calculated to be 1665 kips (7410 kN), which corresponds to a *CF* of 2.53. Consequently, the cap beam was found to be safe, as expected, with a 78% reserve capacity.

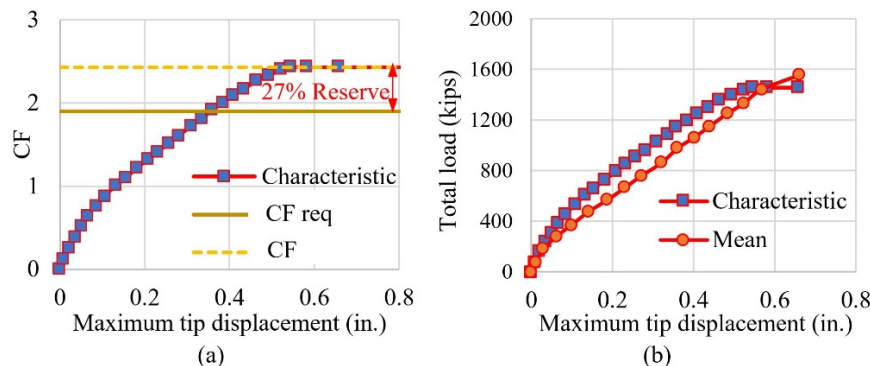


Fig 10—Response of Bridge 1 for (a) Stage 1 and (b) Stage 2; 1 in. = 25.4 mm and 1 kip = 4.45 kN

The methodology was applied, in a similar manner, to the remaining four bridges. The models for each bent beam are shown in Figure 11(a). Shear and flexural crack patterns at the failure conditions are presented in Figure 11(b). Initial cracks typically occurred at the mid-span bottom faces of interior spans as flexural cracks. With the increase in loading, more cracks formed, and the widths of the existing cracks increased. Diagonal compression struts formed in the beams, which represent the deep beam strut action (i.e., shear cracks spanned from the point loads to the column supports). Vertical flexural cracks formed above the column regions, with yielding of the top rebar at those locations. The conditions of the top and bottom reinforcement of the beam are also shown in Figure 11(c). From the cracking pattern, it is clear that the bridge bents are shear critical at the cantilever spans and inner spans near the columns. The yielding of the top and bottom flexural reinforcement of the bridge bent at the beam-column interface caused crushing of the concrete, resulting in a shear-flexural failure mode.

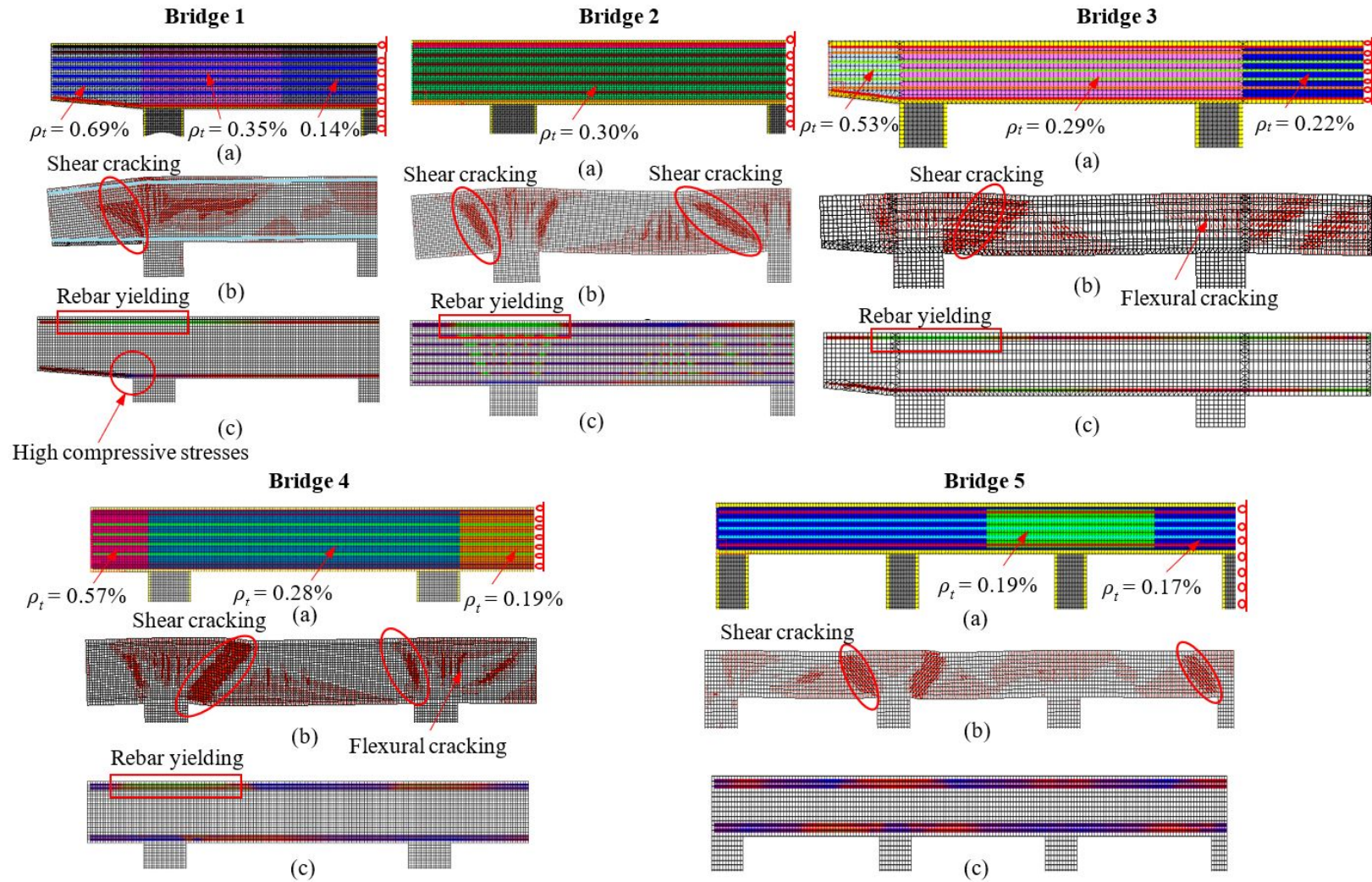


Fig.11—(a) Finite element model developed, (b) crack pattern (10 times actual deflection) and (c) rebar stresses at failure for Bridges 1 through 5

The combined results for all five bridges indicate that all of the bridges are safe in both stage assessments under the existing loading condition. The material resistance factors used in Stage 1 (see Eqns. 2 and 3 in Figure 6) were typically conservative and provided a higher required capacity factor as shown in Table 3. On the other hand, Stage 2 does not consider material resistance factors to determine the required capacity factor, which resulted in a lower required capacity factor as shown in Table 3. Thus, Stage 2 provided a less-conservative assessment approach and, consequently, higher reserve capacities for all of the bridge bents analyzed in this study.

Table 3—Strength evaluation results of deep bridge bents

| Bridge Name | Capacity (kips) | CF_{req} | CF | Stage 1 Reserve | CF_{req} | CF | Stage 2 Reserve |
|-------------|-----------------|------------|------|-----------------|------------|------|-----------------|
| Bridge 1 | 1456 | 1.90 | 2.41 | 27% | 1.42 | 2.53 | 78% |
| Bridge 2 | 2976 | 1.89 | 4.12 | 118% | 1.42 | 4.21 | 196% |
| Bridge 3 | 2565 | 1.89 | 3.18 | 68% | 1.41 | 3.42 | 142% |
| Bridge 4 | 2340 | 1.94 | 2.97 | 53% | 1.46 | 2.87 | 97% |
| Bridge 5 | 3885 | 1.91 | 2.36 | 24% | 1.43 | 2.54 | 77% |

NOTE: 1 kip = 4.45 kN

COMPARISONS WITH SECTIONAL AND STRUT-AND-TIE METHODS

Bridge pier caps are commonly designed using the sectional method, even though this method cannot account for the deep beam action. To demonstrate the capacities obtained, the five bent beams analyzed with the NLFEA were also analyzed using the sectional method. The moment and shear capacities were determined at the critical sections based on the AASHTO LRFD (2017) code. The sectional analysis results indicated that all beams were significantly overloaded in shear. The proposed NLFEA methodology, on the other hand, found significant reserve shear capacities for the same beams by predicting 2.5-times the shear capacity, on average, compared to that obtained from the sectional method as shown in Figure 12(a).

The same bent beams were also analyzed using the strut-and-tie-method (STM) (Scott et al. 2012), using the computer program STM-CAP (Baniya et al. 2018), which is a Visual Basic Advanced (VBA)-based graphical computer program developed specifically for pier caps. Figure 12(b) shows the ratio between the capacities calculated by the NLFEA and the STM. While STM provided larger capacities than the sectional method, the predicted capacities were still much smaller than the proposed NLFEA methodology. The proposed NLFEA methodology predicted 1.5-times the shear capacity, on average, compared to that obtained from STM as shown in Figure 12(b).

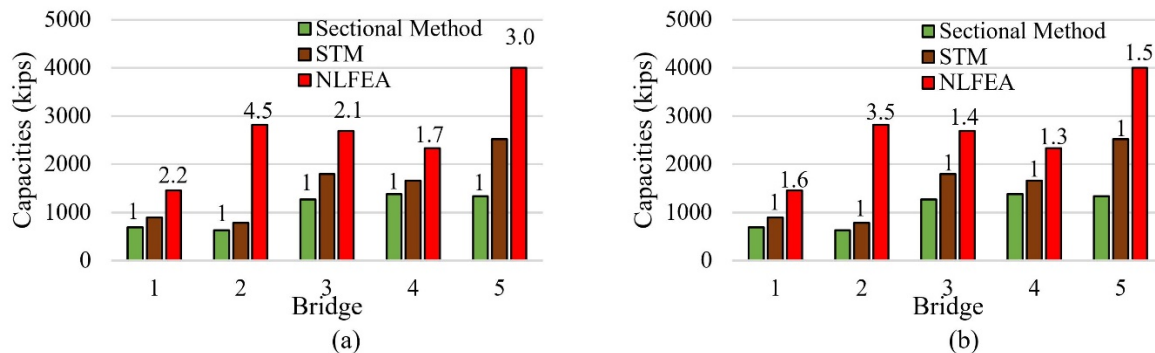


Fig. 12—Comparison of shear capacities from NLFEA with (a) sectional method and (b) STM; 1 kip = 4.45 kN

Figure 13 shows the capacities and the load-displacement responses obtained from all three methods. For the purpose of comparison, the capacities are normalized to the capacities obtained from the sectional method. In most cases, the

pushover responses exhibit an initial linear portion with high stiffnesses followed by nonlinear responses due to concrete cracking and steel yielding. When comparing the calculated capacities of the sectional and STM methods with the pushover curve and failure modes of the NLFEA, results in Figure 13 show that the sectional method predicts the capacities shortly after the linear-elastic region, while the STM predictions are based on either the first yielding of reinforcement or first local crushing of the concrete. Both methods neglect the strain hardening behavior of reinforcement and the re-distribution of stresses due to concrete cracking and reinforcement yielding.

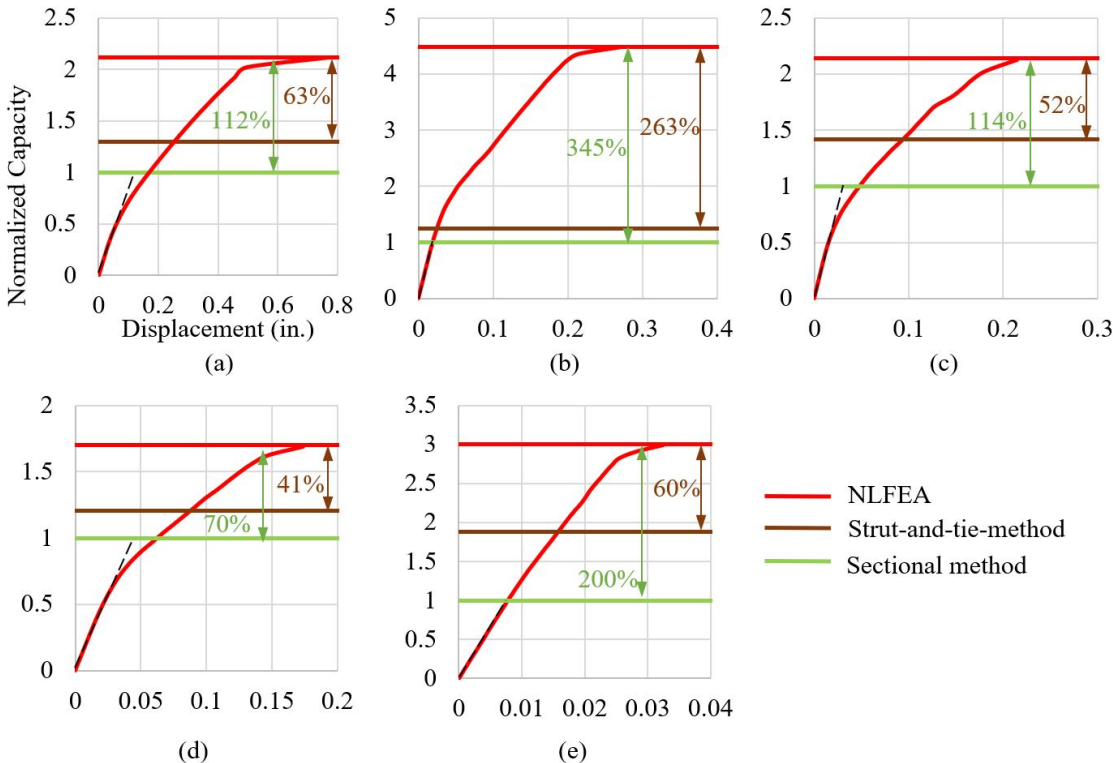


Fig. 13—Load displacement response of (a) Bridge 1, (b) Bridge 2, (c) Bridge 3, (d) Bridge 4 and (e) Bridge 5; 1 in. = 25.4 mm

SIMULATION OF LOAD REDISTRIBUTION

In all of the beams examined, it was found that the failure did not occur at the first yield of reinforcement or first crushing of concrete. There was a significant redistribution of the stresses, which subsequently provided higher load capacities. Bridge 2, for example, showed significant load re-distribution, which resulted in higher differences in the load capacity as compared to the sectional method and STM, as seen in Figure 13(b). The crack patterns and the rebar stresses in the top and bottom reinforcement bars are shown in Figure 14 for the initial, first major damage and failure conditions. Cracks initially formed at mid-span as shown in Figure 14(a). Diagonal cracks did not form during the elastic part of the response. The sectional method considered the failure at the critical sections during this stage, which was overly conservative. However, in the NLFEA, the stresses in the main longitudinal reinforcement kept increasing and penetrating further into the beam, which prevented any localized failure. As a result, widespread cracks were formed. The capacity indicated by the strut-and-tie-method corresponds to Figure 14(b), where the first rebar yielded. After the top reinforcing bar yielded, 2-times higher load could be supported by the beam until the shearing of the concrete as shown in Figure 14(c). The failure occurred from yielding of the reinforcement and shearing of the concrete along the beam length. Consequently, the proposed NLFEA methodology was useful when investigating the load redistribution and the sequence of nonlinear occurrences.

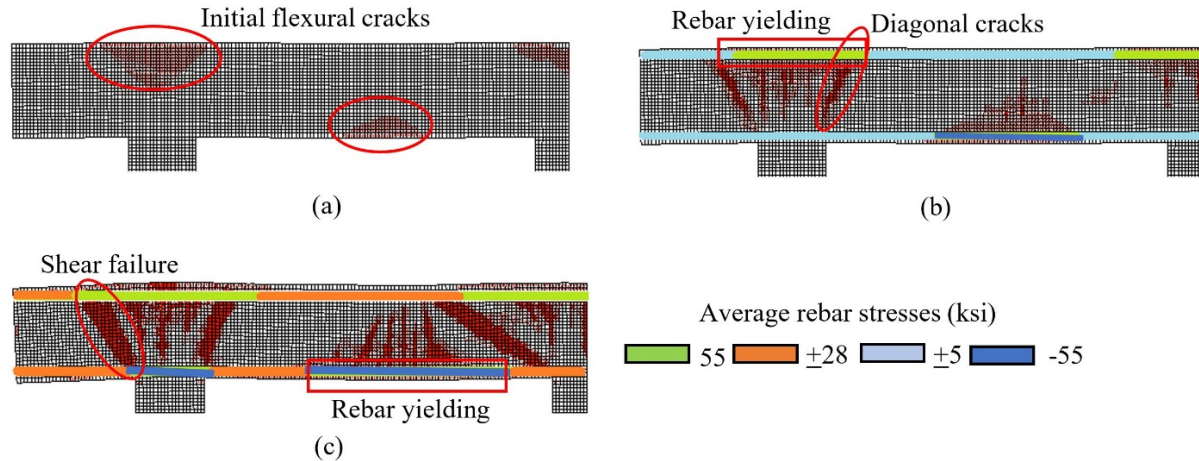


Fig. 14—(a) First cracking, (b) first rebar yielding and (c) failure crack patterns and rebar stresses obtained from the NLFEA for Bridge 2; 1 ksi = 6.9 MPa

SUMMARY AND CONCLUSIONS

A nonlinear finite element analysis (NLFEA) methodology is proposed for the strength evaluation of deep bridge bents. The assessment employs a two-stage safety assessment procedure and considers advanced concrete behaviors such as tension stiffening, compression softening, and dowel action. The application of the proposed methodology is presented by examining five existing bridge bents. The effectiveness of the proposed methodology is discussed and a comparison with sectional and strut-and-tie methods is made. The results of this study support the following conclusions.

1. Most bridge bents are deep beams with nonlinear strain distributions. Analysis methods capable of representing the deep beam action are required to obtain accurate results.
2. The proposed NLFEA methodology was shown to simulate the nonlinear stress/strain distributions, the sequence of nonlinear occurrences and redistribution of forces after concrete cracking and rebar yielding, and the governing failure mechanisms.
3. The proposed two-stage safety assessment procedure simplified the strength assessment process by employing the concept of a capacity factor based on the load and material resistance factors. If the bridge is found overloaded in Stage 1, a more in-depth probabilistic assessment of Stage 2 is required. Stage 2 assessment was shown to predict higher reserve shear capacities than Stage 1 assessment; on average, the difference in capacity was 2-times for the bridges examined in this study.
4. The conventional sectional methods cannot capture the nonlinear strain distribution and thus are not suitable for the analysis of deep beams. The proposed NLFEA methodology predicted 2.5-times the shear capacities, on average, compared to the sectional analyses (performed for demonstrative purposes).
5. The strut-and-tie method was found to provide a strength prediction corresponding to the first yielding of the reinforcement or first crushing on the concrete, without accounting for any force redistribution. The proposed NLFEA methodology predicted 1.5-times the shear capacities, on average, compared to the strut-and-tie analyses.
6. The proposed NLFEA methodology was useful when investigating the load redistribution and the sequence of nonlinear occurrences. Redistribution of the stresses with the subsequent development of nonlinear occurrences was found to provide 2-times the load capacity for one of the bridge bents investigated.
7. There is limited public funding for the rehabilitation and strengthening of the existing bridges. NLFEA that considers the required material models offers the potential to correctly identify and rank overloaded bridges so that available funds can be directed to the most critical bridges.

ACKNOWLEDGMENTS

The authors would like to thank the Ohio Department of Transportation for providing the structural design drawings and PhD candidate Rafael A. Salgado and MS candidates Pappu Baniya, Sálvio A. Almeida Jr., and Sundar Chiluwal, at the University of Toledo, for their feedback and support in this study.

NOTATION

| | |
|------------|--|
| a/d | Shear span-to-depth ratio |
| α_R | Sensitivity factor for the resistance reliability |
| A_b | Cross-sectional area of out-of-plane reinforcement |
| A_y | Cross-sectional area of main reinforcement |
| β | Reliability index |
| CF | Capacity factor |
| CF_{req} | Required capacity factor |
| Δ_m | Mid-span displacement in the beam |
| d | Depth of beam |
| f_c | Concrete characteristic uniaxial compressive strength |
| f_{cm} | Concrete mean uniaxial compressive strength |
| f_s | Reinforcement rupture strength |
| f_y | Reinforcement characteristic yield strength |
| f_{ym} | Reinforcement mean yield strength |
| L_d | Factored loads |
| L_S | Unfactored (service) loads |
| Φ_f | Flexural-behavior reduction factor |
| Φ_S | Shear-behavior reduction factor |
| ρ_t | Reinforcement ratio |
| R_d | Design resistance |
| R_k | Resistance obtained using characteristic material properties |
| R_m | Resistance obtained using mean material properties |
| γ_G | Reduction factor |
| S_t | Spacing of stirrups |
| V_R | Coefficient of variation of resistance |
| w | Width of beam (average) |
| W_c | Width of beam cross-section |

REFERENCES

- AASHTO. 2017. "LRFD bridge design specifications", Customary US units, 8th Edition. American Association of State Highway and Transportation Officials, Washington, DC, 1755.
- ACI Committee 318. 2019. "Building code requirements for structural concrete (ACI 318-19) and Commentary", American Concrete Institute, Farmington Hills, MI, 623.
- Alsaeq, H.M. 2013. "Effects of opening shape and location on the structural strength of RC deep beams with openings", In *Proceedings of World Academy of Science, Engineering and Technology*, 7(6), 494-499.
- Akkaya, Y., Guner, S., and Vecchio, F.J. 2019. "Constitutive model for the inelastic buckling behavior of reinforcing bars", *ACI Structural Journal*, 116(3), 195-204. Retrieved from https://www.utoledo.edu/engineering/faculty/serhan-guner/docs/JP11_Akkaya_et_al_2019.pdf
- Barbachyn, S.M., Kurama, Y.C., and Novak, L.C. 2012. "Analytical evaluation of diagonally reinforced concrete coupling beams under lateral loads", *ACI Structural Journal*, 109(4), 497.
- Baniya, P., Sharma, A., and Guner, S. 2018. "Evaluation of reserve shear capacities of bridge pier caps using the deep beam theory", Final Project Report, Ohio Department of Transportation, Columbus, 120. Retrieved from <http://www.utoledo.edu/engineering/faculty/serhan-guner/STM-CAP.html>
- Baniya, P., and Guner, S. 2019. "Specialized strut-and-tie method for rapid strength prediction of bridge pier caps", *Engineering Structures*, 198, 1-9. Retrieved from http://www.utoledo.edu/engineering/faculty/serhan-guner/docs/JP13_Baniya_Guner_2019.pdf
- Bunni, N.G., Scott, B., Park, R., and Priestley, M. 1982. "Stress-strain behavior of concrete confined by overlapping hoops at low and high strain rates", *Journal of American Concrete Institute*, 79(6), 496-498.
- CSA. 2014. "Design of concrete structures (CSA A23.3-14)", 6th Ed. Canadian Standards Association, Mississauga, Ontario, Canada, 290.
- Cervenka, V. 2008. "Global safety format for nonlinear calculation of reinforced concrete", *Beton-und Stahlbetonbau*, 103(S1), 37-42.
- Clark, A.P. 1951. "Diagonal tension in reinforced concrete beams", *Journal Proceedings*, 48(10), 145-156.

- Collins, M.P., and Mitchell, D. 1991. "Prestressed concrete structures", Response Publications, reprinted in 1997, Canada, 766 pp.
- Demir, A., Ozturk, H., and Dok, G. 2016. "3D numerical modeling of RC deep beam behavior by nonlinear finite element analysis", *Disaster Science and Engineering*, 2(1), 13-18.
- Gandomi, A.H., Alavi, A.H., Shadmehri, D.M., and Sahab, M.G. 2013. "An empirical model for shear capacity of RC deep beams using genetic-simulated annealing", *Archives of Civil and Mechanical Engrg.*, 13(3), 354-369.
- Guner, S., and Vecchio, F.J. 2010. "Pushover analysis of shear-critical frames: formulation", *ACI Structural Journal*, 107(01), 63-71. Retrieved from https://www.utoledo.edu/engineering/faculty/serhan-guner/docs/JP1_Guner_Vecchio_2010a.pdf
- Hwang, S.J., and Lee, H.J. 2002. "Strength prediction for discontinuity regions by softened strut-and-tie model", *Journal of Structural Engineering*, 128(12), 1519-1526.
- Kani, G. 1967. "How safe are our large reinforced concrete beams?", *Journal Proceedings*, 64(3), 128-141.
- Kim, H.S., Lee, M.S., and Shin, Y.S. 2011. "Structural behaviors of deep RC beams under combined axial and bending force", *Procedia Engineering*, 14, 2212-18.
- Niranjan, B.R., and Patil, S.S. 2012. "Analysis of R.C deep beam by finite element method", *International Journal of Modern Engineering Research (IJMER)*, 2(6), 4664-4667.
- Oh, J.K., and Shin, S.W. 2001. "Shear strength of reinforced high-strength concrete deep beams", *Structural Journal*, 98(2), 164-173.
- Özcan, D.M., Bayraktar, A., Şahin, A., Haktanir, T., and Türker, T. 2009. "Experimental and finite element analysis on the steel fiber-reinforced concrete (SFRC) beams ultimate behavior", *Construction and Building Materials*, 23(2), 1064-1077.
- Pan, Z., Guner, S., and Vecchio, F.J. 2017. "Modeling of interior beam-column joints for nonlinear analysis of reinforced concrete frames", *Engineering Structures*, 142, 182-191. Retrieved from http://www.utoledo.edu/engineering/faculty/serhan-guner/docs/JP7_Pan_et_al_2017.pdf
- Popovics, S. 1973. "A numerical approach to the complete stress-strain curve of concrete", *Cement and Concrete Research*, 3(5), 583-599.
- Quintero-Febres, C.G., Parra-Montesinos, G., and Wight, J.K. 2006. "Strength of struts in deep concrete members designed using strut-and-tie method", *ACI Structural Journal*, 103(4), 577.
- Rogowsky, D.M., and MacGregor, J.G. 1986. "Design of reinforced concrete deep beams", *Concrete International*, 8(8), 49-58.
- Salgado, R.A., and Guner, S. 2018a. "A comparative study on nonlinear models for performance-based earthquake engineering", *Engineering Structures*, 172, 382-391. Retrieved from https://www.utoledo.edu/engineering/faculty/serhan-guner/docs/JP10_Salgado_Guner_2018.pdf
- Salgado, R.A., and Guner, S. 2018b. "A numerical analysis methodology for deep cap beams retrofitted with fiber reinforced polymers", *Advances in Concrete Bridges*, ACI Special Publication, SP-333-1, 1-10.
- Schlaich, J., Shafer, K., and Jennewein, M. 1987. "Toward a consistent design of structural concrete", *PCI Journal*, 32(3), 171-179.
- Schlaich, J., and Shafer, K. 1991. "Design and detailing of structural concrete using strut-and-tie models", *Structural Engineer*, 69(6), 113-125.
- Scott, R.M., Mander, J.B., and Bracci, J.M. 2012. "Compatibility strut-and-tie modeling: Part I-Formulation", *ACI Structural Journal*, 109(5), 635.
- Senturk, A.E., and Higgins, C. 2010a. "Evaluation of RCDG bridge bent caps with 1950's Vintage Details - Analytical Methods", *ACI Structural Journal*, 107(5), 544-553.
- Senturk, A.E., and Higgins, C. 2010b. "Evaluation of RCDG bridge bent caps with 1950's Vintage Details – Laboratory Tests", *ACI Structural Journal*, 107(5), 534-543.
- Senturk, A.E. 2008. "Experimental and analytical evaluation of conventionally reinforced deck-girder bridge bent caps with vintage details", PhD Dissertation, Oregon State University, 351.
- Tan, K.H., Kong, F.K., Teng, S., and Weng, L.W. 1997. "Effect of web reinforcement on high-strength concrete deep beams", *Structural Journal*, 94(5), 572-582.
- Vecchio, F.J., and Collins, M.P. 1986. "The modified compression-field theory for reinforced concrete elements subjected to shear", *ACI Journal*, 83(2), 219-231.
- Vecchio, F.J. 2000. "Disturbed stress field model for reinforced concrete: formulation", *Journal of Structural Engineering*, ASCE, 126(9), 1070-1077.
- Wong, P.S., Vecchio, F.J., and Trommels, H. 2013. "VecTor2 and FormWorks user's manual", Technical Report, Department of Civil Engineering, University of Toronto, 347. Retrieved from http://www.vectoranalysisgroup.com/user_manuals/manual11.pdf

ACI member **Anish Sharma** is an MS student at the University of Toledo. He received his B.Sc. degree in 2014 from the Institute of Engineering, Tribhuvan University (Nepal). His research interests include finite element analysis and load rating of deep concrete beams and foundations.

ACI member **Serhan Guner** is an Assistant Professor in the Department of Civil and Environmental Engineering at the University of Toledo, OH. He received his Ph.D. from the University of Toronto, ON, Canada. He is a member of Joint ACI-ASCE Committee 447, Finite Element Analysis of Reinforced Concrete Structures, ACI Committee 370: Blast and Impact Load Effects, and ACI Committee 123: Research and Current Developments. His research interests include computational mechanics, numerical modeling, shear and torsion, response to extreme loads, deep beams and disturbed regions, and creation of analysis tools and software.